Advances in Geo-Energy Research

Vol. 18, No. 2, p. 202-206, 2025

Short communication

Unlocking the shiny surface features of shale shear fractures at micro-nanoscale

Hongjian Zhu[1,2], Bo Qi[2], Jianhui Li[3], Cai Li[1], Ali Raza[4], Chaobin Guo[1]*

[1]*Technology Innovation Center for Carbon Sequestration and Geological Energy Storage, Ministry of Natural Resources, Chinese Academy of Geological Sciences, Beijing 100037, P. R. China*

[2]*School of Vehicle and Energy, Yanshan University, Qinhuangdao 066000, P. R. China*

[3]*Oil and Gas Technology Institute, Changqing Oilfield Company, Xi'an 710018, P. R. China*

[4]*Department of Earth and Atmospheric Sciences, University of Houston, Houston TX 77204, USA*

Keywords:
Shale
shear deformation
fracture mirror
clay
graphitization

Cited as:
Zhu, H., Qi, B., Li, J., Li, C., Raza, A., Guo, C. Unlocking the shiny surface features of shale shear fractures at micro-nanoscale. Advances in Geo-Energy Research, 2025, 18(2): 202-206.
https://doi.org/10.46690/ager.2025.11.10

Abstract:
Shale shear fracture mirrors are key indicators of localized shear deformation, yet their high reflectivity origin remains unclear. This study employs electron microscopy and Raman spectroscopy to analyze fracture mirrors from the Lower Cambrian Qiongzhusi shale. Results reveal the shiny surface is not merely a product of mechanical polishing but is primarily attributed to the formation of highly ordered nanocoatings on fracture surface. The coatings comprise aligned clay minerals and, crucially, organic materials that have undergone shear-induced partial graphitization. Transmission electron microscopy reveals a about 0.46 nm lattice fringe spacing, and Raman spectroscopy confirms a moderate structural order and an elevated thermal maturity of organic matter. This transformation yields a dense material dominated by ultra-micropores, which minimizes light scattering of fracture surface. The formation of fracture mirrors results from shear displacement and frictional heating, which lead to mechanical comminution and microstructural reorganization. This finding establishes the shear fracture mirrors as the key indicators for revealing bedding-parallel slip history in shale-involved detachment and, more practically, for assessing fluid migration pathways, seal integrity, and natural fracture networks in shale gas systems.

1. Introduction

Fault mirrors (or fracture mirrors) are reliable indicators of frictional sliding within rock masses. They are associated with a variety of geological activities, such as seismic events, fault slip, landslides, and glacial movement (Schleicher et al., 2010; Siman-Tov et al., 2013). They are characterized by naturally polished, highly reflective, glossy surfaces with a distinct metallic or vitreous luster under visible light, creating a contrast against the surrounding rocks (Verberne et al., 2014). Geological records indicate that fault mirrors are ubiquitously developed within fault zones intersecting sedimentary sequences (e.g., mudstones, shales, coals, sandstones, limestones) as well as granite and hematite (Siman-Tov et al., 2013; Zhu et al., 2025). Their geometry shows a significant correlation with fault slip trajectories, endowing them with important implications for understanding the dynamics of faulting or fracturing processes. Simulations of low- to high-velocity rock friction confirm that fault mirrors develop across a wide range of shear rates, representing conditions from plate motion to seismic slip (Kuo et al., 2014). The resultant mirror-like surfaces can achieve an average roughness as low as 100 nm (Siman-Tov et al., 2013). Over recent decades, several mechanisms have been proposed to explain the formation of fault mirrors, including mechanical polishing, smearing,

Yandy Scientific Press

*Corresponding author.
E-mail address: zhj8641@163.com (H. Zhu); q268962911@163.com (B. Qi); ljhui_cq@petrochina.com.cn (J. Li); licai@cags.ac.cn (C. Li); araza22@cougarnet.uh.edu (A. Raza); guochaobin123@hotmail.com (C. Guo).

Received September 29, 2025; revised October 20, 2025; accepted October 29, 2025; available online November 2, 2025.

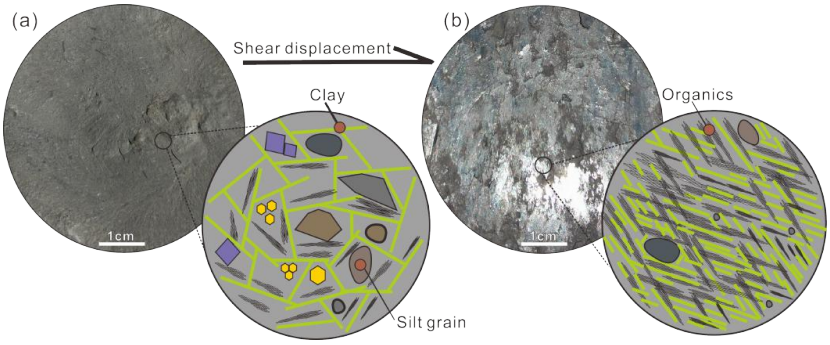

Fig. 1. Schematic model illustrating the evolution of a coarse fracture surface into a naturally polished SSFMs through shear displacement or deformation. (a) The coarse fracture surface composed of loosely packed and randomly oriented grains (e.g., clay, organics, silt and (b) after shear slip, the fracture surface becomes smooth and shiny. The process involves the comminution, reorientation, and smearing of grains to form tightly packed and directionally oriented nanocoatings (or naturally polished films), with striations indicative of the shear direction.

frictional melting, precipitation of hydrothermal minerals, and nanocoatings formed by platy particles such as clay minerals and graphite (Schleicher et al., 2010; Kuo et al., 2014).

As a widely distributed and laminated sedimentary rock in the upper crust, shale is prone to interlayer slip along bedding planes under shear stresses (Aydin and Engelder, 2014; Yang et al., 2021; Cai et al., 2024; Li et al., 2025; Wu et al., 2025). During slip, the interfacial material undergoes intense shear deformation and frictional heating, producing an ultra-thin, micro- to nano-scale coatings that smoothen the fracture surface into mirrors (Fig. 1). Research on shale shear fracture mirrors (SSFMs) has advanced our understanding of their basic optical, morphological, and fabric characteristics, as well as their formation mechanisms (Schleicher et al., 2010; Cai et al., 2025), thereby providing insights into their controls on hydrocarbons migration, seal integrity, and natural fracture networks in shale gas systems. Zhu et al. (2024) and Zhu et al. (2025) identified typical SSFMs within the detachment layers of the Wufeng-Longmaxi Formation and Qiongzhusi Formation in the Sichuan Basin, South China. They investigated their microstructures and geological implications for shale gas preservation by analyzing the pore-fracture systems at micro-nanoscale. Nevertheless, the coupling effects between the uniquely enriched coatings and the mirror-like surfaces, along with the microstructural evolution of the rock at the interface under thermo-shear conditions, remain unresolved.

This study integrates high-resolution electron microscopy and Raman spectroscopy to conduct a fine-scale characterization of SSFMs. The aim is to elucidate their micro-nanoscale structural characteristics and evolutionary processes, thereby investigating the mechanisms of their high surface reflectivity.

2. Sample and methods

This study focuses on shale samples from the Lower Cambrian Qiongzhusi Formation in the Sichuan Basin. Recognized as a key detachment layer during the tectonic evolution of basin, the deformation behavior of this organic-rich shale was enabled by its unique mechanical properties. These properties, stemming from a combination of abundant brittle minerals, well-developed laminations, organic matter, and clay minerals, facilitated ductile deformation under shear stress, which in turn controlled the development of the peripheral fold-thrust belts (Zhu et al., 2025).

The microstructural characteristics of the SSFMs were analyzed using a combination of electron microscopy and atomic force microscopy (AFM). Microscale features were imaged with a scanning electron microscope (SEM; FEI Quanta 200F, Zeiss Gemini 450), while nanoscale details were resolved using transmission electron microscopy (TEM; JEM-2100F). Furthermore, the surface topography of a representative shiny area was scanned with an AFM (SPA-400) over a $5\,\mu m \times 5\,\mu m$ area. The accompanying software was used to calculate standard roughness parameters, including the root-mean-square (RMS) roughness and the roughness average, across the entire scanned region. Micro-Raman spectroscopy was performed using a Horiba LabRAM HR Evolution confocal Raman microscope at the Chinese Academy of Geological Sciences. The Raman spectral data were utilized to assess the thermal maturity and the graphitization degree of the organic matter. The Raman maturity (R_0) was calculated based on:

$$R_0 = 0.0537\,d(G-D) - 11.21 \quad (1)$$

where $d(G-D)$ is the distance between the G and D bands in wavenumbers (cm^{-1}).

The degree of graphitization was quantitatively evaluated by the intensity ratio of the D-band to the G-band (I_D/I_G).

3. Results and discussion

Multi-scale observations of the SSFMs reveal its transition from a macroscopically glossy surface to nanoscale constituents, including aligned clay minerals, organic grains, and their composites (Fig. 2). The images show that the mirror-like surface is a direct consequence of the highly ordered micro-nanoscale structures generated by intense shear. At the macroscopic scale, the SSFMs exhibit a distinct, highly reflective zone (Fig. 2(a)), contrasting sharply with the surrounding rough matrix. As the magnification increases to the microscopic level, the seemingly uniform glossy surface resolves

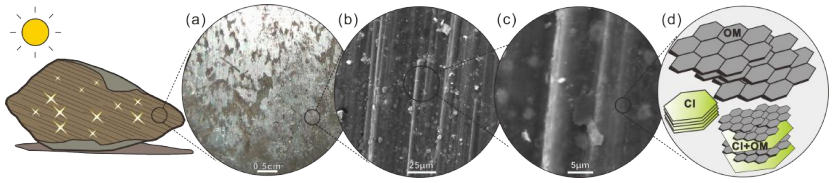

Fig. 2. Multi-scale structural characterization of the SSFMs from macroscopic to nanoscale (modified from Zhu et al. (2024)). Clay-organic composite is labelled "Cl+OM", organic matter is labelled "OM", and clay is labelled "Cl".

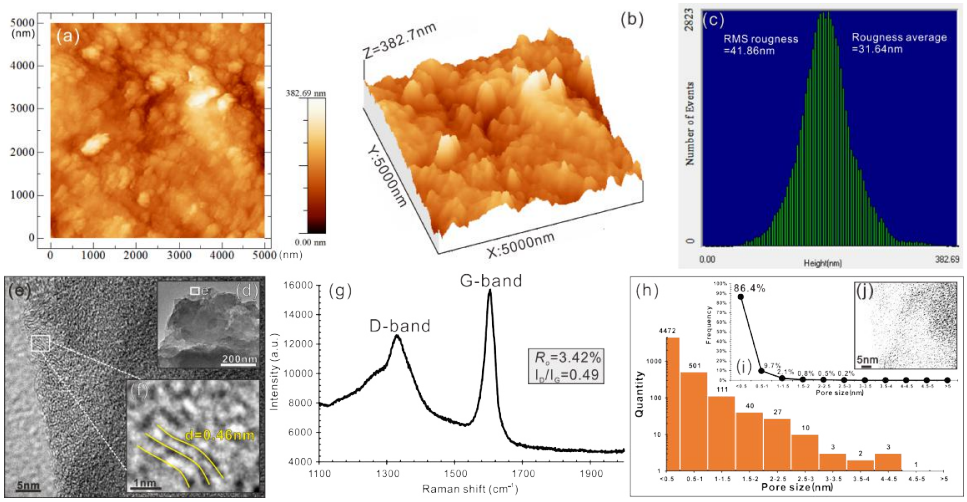

Fig. 3. Nano-scale characterization of the SSFMs. (a) 2D AFM image showing the height map of SSFMs, (b) 3D AFM image showing the height map of SSFMs, (c) Statistical height information map, (d, e) TEM images revealing the nanostructures of organic matter, (f) TEM image indicating a lattice fringe spacing of 0.46 nm, (g) Raman spectrum with the Ro of 3.42% and the I_D/I_G ratio of 0.49. (h) Pore size distribution histogram of the organic nanopores, (i) Frequency curve of organic nanopores with different pore sizes, (j) Binary image highlighting the organic nanopores.

into a series of well-aligned, sub-parallel striations (Figs. 2(b) and 2(c)). These striations are the surface expression of the extreme shear deformation, indicating a predominant slip direction and the smearing of materials (Zhu et al., 2025). The schematic representation deconstructs this final product of nanocoatings (Fig. 2(d)), identifying three key components: well-ordered organic matter, clay, and clay-organic composite.

In surface optics, the mirror-like reflectivity is fundamentally governed by surface roughness at the scale of the incident light wavelength (typically hundreds of nanometers for visible light). When the RMS roughness is significantly smaller than the light wavelength, light scattering is minimized, and most of the incident light is reflected specularly, resulting in a shiny appearance (Siman-Tov et al., 2013). The AFM quantitatively demonstrates that the SSFMs possess the exceptionally low RMS and average roughness values of 41.86 nm and 31.64 nm (Figs. 3(a)-3(c)), respectively, which is more than an order of magnitude smaller than the wavelength of visible light. This ultra-low nanoscale roughness, resulting from the formation of the dense and continuous nanocoatings, is the direct reason for the high optical reflectivity observed by the naked eye and in optical photographs (Fig. 2(a)).

The SEM images reveal a smooth and continuous surface at the micron scale, which is the direct cause of the high optical reflectivity (Fig. 2). At higher magnification, the TEM images show that the organic materials in the coatings possess a distinct laminated nanostructure in local areas (Figs. 3(d) and 3(e)). Further investigation by high-resolution TEM (Fig. 3(f)) reveals lattice fringes with a measured spacing of approximately 0.46 nm. The interlayer spacing of graphite is approximately 0.335 nm (3.35 Å), representing the typical distance between adjacent carbon layers in its crystalline structure. These layers are held together by van der Waals forces, whereas the carbon atoms within each layer are bonded by strong covalent bonds (Kuo et al., 2014). Therefore, the presence of organic carbon in the nanocoatings of SSFMs, coupled with the observed structural data, indicates that the organic carbon did not undergo complete graphitization. However, this value is notably smaller than the typical interlayer spacing of immature amorphous carbon but approaches that of turbostratic carbon (Galvez et al., 2013), indicating a significant degree of structural ordering. This finding is supported by the Raman spectroscopy results (Fig. 3(g)). The spectrum displays characteristic D and G bands, and the calculated I_D/I_G ratio of 0.49 signifies a moderately ordered carbon structure, consistent with a calculated Ro of 3.42%. This confirms that the organic matter has undergone partial graphitization, likely facilitated by the combined effects of shear stress and frictional heating during bedding-parallel slip in the shale-involved detachment systems.

The organic nanoporosity is another important factor to reflect its graphitization degree. Previous studies have shown

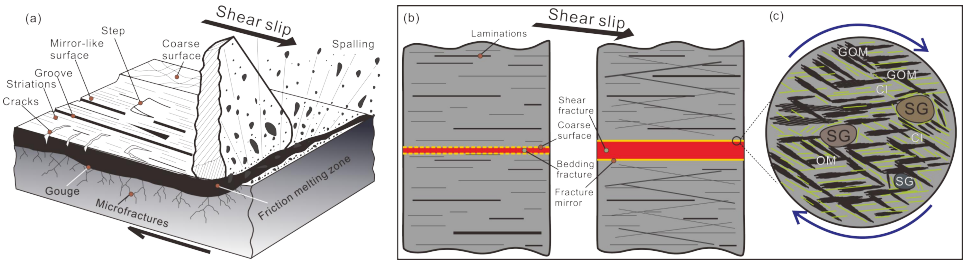

Fig. 4. (a) Schematic representation of interplay of mechanical fragmentation and thermal effects leading to SSFMs formation and the fracture surface gloss development (modified from Spray, 1989) and (b, c) The formation and structural evolution of fracture mirrors are revealed from macro to micro scales. Graphitized organic matter is labelled "GOM", organic matter is labelled "OM", clay is labelled "Cl", and silt grain is labelled "SG".

that the porosity is significantly reduced in graphitized organic matter (Hou et al., 2024; Yang et al., 2025). The sponge-like pore structure disappears, with most mesopores and macropores being transformed into micropores. Furthermore, these pores are largely isolated (dead pores) with poor connectivity. The pore size distribution demonstrates that more than 96% of the organic nanopores are smaller than 1 nm (Figs. 3(h) and 3(i)). These extremely fine micropores, visible as dark contrast in the binary image (Fig. 3(j)), results from the dense packing of the graphitized carbon nanostructures.

Therefore, the high reflectivity of the SSFMs is not a result of simple mechanical polishing but is attributed to the formation of a continuous, dense, and highly ordered nanocoatings on the slip surface. It is worth noting that the existence of clay-rich nanocoatings on SSFMs from clay-rich, organic-lean mudrocks has been extensively studied and largely recognized (Schleicher et al., 2010). In contrast, the laminated or layered organic carbon structures found in the coatings of SSFMs have gotten relatively less attention. This coating consisting some graphitized carbon materials is characterized by a well-developed laminated nanostructure with advanced thermal maturity and a predominance of ultra-micropores (pore size less than 1 nm), all of which minimize light scattering and create a specularly reflective surface.

Mudstones and shales within active fault zones commonly exhibit anomalous increases in vitrinite reflectance, enhanced graphitization of organic carbon, and enrichment of graphitic carbon components (Hou et al., 2024; Zhu et al., 2025). This phenomenon is closely associated with the mechano-chemical transformation of organic carbon, driven by the combined effects of shear deformation and frictional heating during fault slip. This process promotes the irreversible transformation of low-density, structurally disordered amorphous carbon into high-density, structurally ordered crystalline graphite, resulting in the formation of chemically inert graphite. For instance, fault mirrors exposed after the Wenchuan earthquake predominantly developed in the Upper Triassic Xujiahe Formation carbonaceous mudstone (Kuo et al., 2014). The carbon content in the principal slip zone and along the slip surfaces is significantly higher than that of the surrounding rocks. Moreover, graphite crystals approximately 50 nm in size have been identified within the principal slip zone. Friction experiments simulating coseismic conditions (~1 m/s) have confirmed that these crystals are products of coseismic frictional graphitization (Kuo et al., 2014; Kuo et al., 2017). In the fields of seismology and tribology, the low-friction characteristics exhibited by graphite-based materials during friction primarily stem from their unique layered crystal structure and the consequent interlayer shear slip behavior (Kuo et al., 2017). The crystal structure of graphite consists of stacked planes of carbon atoms, with adjacent layers bonded by weak van der Waals forces. This pronounced anisotropy endows graphite with extremely low interlayer shear strength. Consequently, the enrichment of graphitic carbon components along SSFMs can facilitate subsequent phases of fault deformation.

Evidence indicates that the intense shear stress and frictional heating during fault slip did not merely cause comminution and mechanical polishing but, more importantly, triggered the nanostructural reorganization of the inherent organic matter and clay minerals. The schematic diagram elucidates a mechanism inherent to shale shear slip, driven by the interplay of mechanical fragmentation and thermal effects (Fig. 4) (Spray, 1989). The shear slip in shale detachment systems preferentially utilizes the pre-existing bedding planes (Zhu et al., 2025), and these planes act as inherent weaknesses, dictating the initial location and orientation of the fractures that evolve into SSFMs (Fig. 4(b)). The process initiates with cataclasis (particle breakage) and frictional melting along the slip surface (Fig. 4(a)), which collectively induce the preferential alignment of platy and ductile constituents, notably clay minerals, organic matter, as well as the clay-organic composites (Figs. 4(b) and 4(c)). Concurrently, frictional heating significantly elevates the local temperature, facilitating the incipient graphitization of the organic component. The newly formed graphitic carbon, characterized by its pronounced layered structure, acts as a solid lubricant. This, in turn, reduces the frictional resistance along the slip plane, thereby promoting further slip localization and enhancing the development of a characteristic mirror-like surface gloss. Note that the presence of a graphitized carbon nanostructure is a diagnostic feature of SSFMs in organic-rich shales. While clay alignment is a fundamental mechanism (Schleicher et al., 2010), organic matter graphitization is also identified as a critical co-agent that significantly enhances the development and reflectivity of the SSFMs in same geological settings (Kuo et al., 2014). The formation of the nanocoatings is the fundamental reason for the high reflectivity of SSFMs. More significantly, the exceptional preferred orientation of these nanocoatings parallel

to the fracture surface minimizes light scattering by eliminating abrupt topographic and compositional heterogeneities. Essentially, the shear process transforms a randomly rough surface into a specularly reflective, nanoscale layered material (Schleicher et al., 2010). This mechanism bridges the gap between the macroscopic observation of shine and the nanoscale structural evolution, providing a material-based explanation for the fracture mirror phenomenon. Its presence is, therefore, a reliable indicator of past localized shear deformation and associated thermal-pressurization conditions, with significant implications for understanding fluid migration pathways and seal integrity in shale gas systems.

4. Conclusions

This study investigates the origin of the shiny features of SSFMs by linking their macroscopic reflectivity to micro-nanoscale structural evolution. The most significant outcomes follow:

(1) The mirror-like surface is a direct result of intense shear deformation generating the densely packed nanocoatings on the shale fracture. The high reflectivity is achieved through two synergistic effects: the extreme mechanical smearing and preferential alignment of platy particles that eliminate surface roughness, and the thermal-driven partial graphitization of organic matter, which produces a nanostructured carbon phase with minimal light-scattering porosity.

(2) The presence of SSFMs, therefore, serves as a reliable geological archive of past localized shear events and associated thermo-mechanical conditions. Understanding this mechanism has significant implications beyond mere visual identification. It provides critical insights into the physico-chemical processes operative during bedding-parallel slip in shale-involved detachment and their profound influence on the evolution of pore-fracture systems. Consequently, recognizing SSFMs is essential for accurately evaluating fluid migration pathways and seal integrity in shale gas reservoirs, ultimately impacting strategies for hydrocarbon exploration and production.

Acknowledgements

The work was supported by the Technology Innovation Center for Carbon Sequestration and Geological Energy Storage, Ministry of Natural Resources, Chinese Academy of Geological Sciences (No. MNRCCUS022301), Hebei Natural Science Foundation (No. D2023203008), National Science and Technology Major Project of China (No. 2025ZD1403901), and National Natural Science Foundation of China (No. 42102186).

Conflict of interest

The authors declare no competing interest.

References

Aydin, M. G., Engelder, T. Revisiting the Hubbert–Rubey pore pressure model for overthrust faulting: Inferences from bedding-parallel detachment surfaces within Middle Devonian gas shale, the Appalachian Basin, USA. Journal of Structural Geology, 2014, 69: 519-537.

Cai, J., Jiao, X., Wang, H., et al. Multiphase fluid-rock interactions and flow behaviors in shale nanopores: A comprehensive review. Earth-Science Reviews, 2024, 257: 104884.

Cai, Z., Liu, Y., Li, J., et al. Nanostructure and evolution of thin shells in brittle-ductile shear zones. Advances in Geo-Energy Research, 2025, 17(1): 56-67.

Galvez, M., Beyssac, O., Martinez, I., et al. Graphite formation by carbonate reduction during subduction. Nature Geoscience, 2013, 6(6): 473-477.

Hou, Y., Yu, R., Li, J., et al. Molecular structure characterization of kerogen in contact metamorphic shales: Insights into the effect of graphitization on organic matter pores. AAPG Bulletin, 2024, 108(4): 633-662.

Kuo, L., Li, H., Smith, S., et al. Gouge graphitization and dynamic fault weakening during the 2008 Mw 7.9 Wenchuan earthquake. Geology, 2014, 42: 47-50.

Kuo, L. W., Di Felice, F., Spagnuolo, E., et al. Fault gouge graphitization as evidence of past seismic slip. Geology, 2017, 45 (11): 979-982.

Li, Z., Xi, K., Niu, X., et al. How bedding-parallel fractures affect fluid activity in a relatively closed lacustrine shales system: Evidence from calcite veins. Marine and Petroleum Geology, 2025, 173: 107276.

Schleicher A. V., van der Pluijm, B. A., Warr, L. N. Nanocoatings of clay and creep of the San Andreas fault at Parkfield, California. Geology, 2010, 38(7): 667-670.

Siman-Tov, S., Aharonov, E., Sagy, A., et al. Nanograins form carbonate fault mirrors. Geology, 2013, 41(6): 703-706.

Spray, J. G. Slickenside formation by surface melting during the mechanical excavation of rock. Journal of Structural Geology, 1989, 11(7): 895-905.

Verberne, B., Pluemper, O., Damd, W., et al. Superplastic nanofibrous slip zones control seismogenic fault friction. Science, 2014, 346: 1342-1344.

Wu, C., Zhu, H., Ju, Y., et al. CO_2 phase fluctuation-induced topological damage enhances shale strength. International Journal of Rock Mechanics and Mining Sciences, 2025, 194: 106206.

Yang, W., Xu, L., Chen, D. X., et al. How argillaceous reservoirs exhibit better quality than silty mudstones? Anomalous behavior of shale gas-bearing properties of continental fine-grained sediments in Southwest China and its possible forcing mechanisms. Petroleum Science, 2021, 18(6): 1589-1610.

Yang, M., Pan, Y., Feng, H., et al. Fractal characteristics of pore structure of Longmaxi shales with different burial depths in southern Sichuan and its geological significance. Fractal and Fractional, 2025, 9(1): 2.

Zhu, H., Lu, Y., Pan, Y., et al. Nanoscale mineralogy and organic structure characterization of shales: Insights via AFM-IR spectroscopy. Advances in Geo-Energy Research, 2024, 13(3): 231-236.

Zhu, H., Ju, Y., Lu, Y., et al. Natural evidence of organic nanostructure transformation of shale during bedding-parallel slip. GSA Bulletin, 2025, 137(5-6): 2719-2746.